

Online Gaussian Process State-Space Models: Learning and Planning for Partially Observable Dynamical Systems

Soon-Seo Park, Young-Jin Park and Han-Lim Choi

Abstract—Gaussian process state-space model (GPSSM) is a probabilistic dynamical system that represents unknown transition and/or measurement models as the Gaussian process (GP). The majority of approaches to learning GPSSM are focused on handling given time series data. However, in most dynamical systems, data required for model learning arrives sequentially and accumulates over time. Storing all the data requires large amounts of memory, and using it for model learning can be computationally infeasible. To overcome this challenge, this paper develops an online inference method for learning the GPSSM (onlineGPSSM) that fuses stochastic variational inference (VI) and online VI. The proposed method can mitigate the computation time issue without catastrophic forgetting and supports adaptation to changes in a system and/or a real environments. Furthermore, we propose a GPSSM-based reinforcement learning (RL) framework for partially observable dynamical systems by combining onlineGPSSM with Bayesian filtering and trajectory optimization algorithms. Numerical examples are presented to demonstrate the applicability of the proposed method.

I. INTRODUCTION

State-Space Models (SSMs) are the most general representation of dynamical systems and have been successfully applied in a variety of applications such as robotics, ecology, finance and neuroscience [1,2]. Typically, SSMs describes a system as a transition model and a measurement model. System identification [3], i.e. learning dynamics models from data, enables unknown transition and/or measurement mapping through parameterized models. The models obtained through system identification can be used to regenerate measurements and predict future measurements as well as control the system [4]–[15].

Algorithms that learn unknown systems need to take several important challenges into consideration. First, the data required to identify the system is often not available before the system interacts with the real environment and can be partially observable and noisy. Secondly, in most dynamical systems, the data arrives sequentially and accumulates over time. Although simply storing all the previous data alleviates the problem, it requires large amounts of memory. Even worse, it is often infeasible in real-world applications where access to the previous data is limited. Also, using all data

for model learning can cause a higher computational load. Lastly, system models can change due to unknown factors such as abrasion, temperature, and humidity, and can be affected by disturbances such as wind. Such unknown factors and disturbances cause the expected system output and the actual output to be different. The difference can degrade the performance of the system and lead to failure.

RL is known as a general machine learning framework that learns and controls unknown system models by interacting with real environments. Model-free RL is one of the approaches to RL that relies on the approximation of the global value function [2,16]. Thus, they typically require complex relational models and a relatively large number of direct interactions with the physical system. In contrast, a model-based RL method was developed to achieve data efficiency as well as control of complex dynamic systems [2,6,8,9,16]–[20], which can also provide better generalization. Over last few years, GP-based control and RL algorithms have gradually drawn attention as they can learn the robust dynamics model with a small number of episodes [6,8,9,17,18]. These GP-based algorithms assume that the states are fully observable and then learn a regression model where the difference between states over time is an output and the state is an input. However, in real systems, the state cannot be measured directly but is inferred from a series of noisy measurements.

Gaussian process state-space model (GPSSM) is a probabilistic dynamical system that represents unknown transition and/or measurement models as a GP [4,11]–[15]. GPSSM is non-parametric, which makes it effective in learning from a small number of time series data that can be partially observable and noisy. By using GPs for latent transitions and/or measurement models, we can get away with an approximate model and learn a distribution over functions. This allows us to account for model uncertainty. Learning the GPSSM is generally intractable due to the nonlinearity and non-Gaussianity of the dynamics model in the latent state. Thus, a number of prior works focus on learning GPSSM from given time series data. A small number of online learning methods directly apply a streaming variational Bayesian (streaming-VB) [21] or use limited memory [12] to handle sequentially arriving data, but they suffer

{sspark, yjpark, hanlimc}@lics.kaist.ac.kr
Preprint. Work in progress.

from catastrophic forgetting.

This paper presents the online inference method for the GPSSM (online GPSSM) that tackles the following key challenges; computation time, catastrophic forgetting and adaptation to changes. The onlineGPSSM fuses stochastic variational inference (VI) [11,22] and online VI [21,23,24]. First, true dynamic is incorporated into the approximate posterior based on stochastic VI, which provides us with a tractable variational approximation of true posterior. When a new measurement arrives, the previous approximate posterior is combined with the new prior and used to obtain a new approximate posterior via the online VI. Critically, the previous approximate posterior constrains the drastic change of the hyperparameters and prevents catastrophic forgetting without revisiting the previous measurement. The proposed method can mitigate the computation time issue without catastrophic forgetting and supports adaptation to changes in a system and/or real environments. Accordingly, our method can be applied to reinforcement learning for partially observable dynamic systems. Similar to GP-based RL frameworks [6,8,17,18], the onlineGPSSM is integrated with trajectory optimization and Bayesian filtering algorithms, which can generate a robust control policy for control/planning. The validity of the proposed method is demonstrated with numerical examples on a synthetic toy and on a fixed-wing unmanned aerial vehicle in a wind field.

II. RELATED WORK

Gaussian Process State-Space Model (GP-SSMs) are one of the most popular class of probabilistic SSMs. Previous works on inference methods for learning the GPSSM can be found in [4,11]–[15]. One class of approaches is to combine sequential Monte Carlo (SMC) with Markov chain Monte Carlo (MCMC) [13,15] or Expectation Maximization (EM) [14]. Although These methods are close to (exact) true distribution, practical use is limited due to its extreme computational burden. This calls for approximations and a promising approach presented by [4,11,14], using inducing points and variational inference framework. For example, Frigola et al. [14] propose a hybrid inference approach combining variational inference and SMC. They approximate the GP by using the sparse variational framework and replace MCMC with a stochastic optimization.

Recently, stochastic optimization based on the reparameterization trick [25] has been successfully applied to the model inference and learning methods. Towards this approach, Eleftheriadis et al. [4] suggest an inference method to approximate the posterior of the latent state with a Markov-structured Gaussian distribution parameterized by a recognition model (i.e., bi-RNN). Doerr et al. [11] propose an inference scheme based on stochastic

variational inference for deep GPs as presented in [22]. They followed a sparse variational approximation and incorporated the true dynamics into the approximate posterior by combining sampling- and gradient-based learning. Specifically, they obtain the approximate posterior distribution (i.e., variational distribution) of latent states by sampling in the true dynamics. Our framework also adopts a stochastic variational inference scheme [22]. However, rather than employing a recognition model to find a informative model initialization [22], the proposed framework obtains an informative prior distribution of the initial state using Bayesian filtering and the results of online learning.

Online learning is a common approach where it is computationally infeasible to learn over an entire data set, which is essential for the learning of a dynamical system in which data arrives sequentially. Using only some of the recent data for model learning causes catastrophic forgetting [12]. Streaming Variational Bayes (Streaming-VB) [21] is known as the most general method to online learning. Applying streaming-VB for online learning of GPSSM is conceptually presented in [14] but not fully explored. However, such a vanilla application of Streaming-VB prevents online updating of hyperparameters in model learning. Consequently, it cannot be free from catastrophic forgetting (More details will be addressed in Section IV-B). To overcome this limitation, we employ the online VI approach that allows for updating of the hyperparameters. Note that online VI has already been successfully utilized in static setting problems such as regression, classification and deep generative models [26,27]. It has yet to be applied to online learning of recurrent state-space models.

The Gaussian process (GP) has been widely used for model-based reinforcement learning and control problems [6,8,9,17,18]. For instance, the work by Deisenroth et al. [9] developed the GP-based policy search framework called PILCO. A number of other methods have been proposed to avoid policy parameterization and reduce computation time [6,8,17,18], where the GP is combined with the trajectory optimization method called Differential Dynamic Programming (DDP). However, such GP-based algorithms assume that the states are fully observable, which may not work well under significant noise [10]. To deal with noisy measurements, an extended version of PILCO is proposed in [10]. They used GPSSM instead of GP for model learning and developed a policy search method through Bayesian filtering. Our RL framework shares some similarities with Probabilistic Differential Dynamic Programming (PDDP) [8] and iterative Linear Quadratic Gaussian in belief space (belief space iLQG) [28]. PDDP learns the system model with fully observable measurements using GP and controls the learned model through it-

erative Linear Quadratic Gaussian Regulator (iLQR). Our framework, however, can learn system models from partially observable and/or noisy measurements. Belief space iLQG assumes a dynamics model is given and the stochasticity comes from the process and sensor noises; however, our framework is a data-driven approach that learns the dynamics model and/or sensor model parameters, and it takes into account the uncertainty of a model using the GPSSM.

III. PRELIMINARIES

A. Problem Formulation

We consider a discrete-time partially observable dynamical system described by:

$$\begin{aligned} \mathbf{x}_{t+1} &= f(\mathbf{x}_t, \mathbf{u}_t) + \mathbf{w}_f, \\ \mathbf{y}_t &= g(\mathbf{x}_t) + \mathbf{w}_g, \end{aligned} \quad (1)$$

where t indexes time, $\mathbf{x} \in \mathbb{R}^D$ is a latent state, $\mathbf{u} \in \mathbb{R}^P$ are control inputs, $\mathbf{y} \in \mathbb{R}^O$ are measurements and $\mathbf{w}_{(\cdot)} \sim \mathcal{N}(\mathbf{0}, \sigma_{(\cdot)}^2 \mathbf{I})$ are the Gaussian system/measurement noise. The transition model f and/or the measurement model g are unknown. In optimal control, as well as in reinforcement learning, the goal is to find the optimal control policy $\pi(\mathbf{x}_t, t)$ that minimizes the expected cost:

$$\mathcal{J}^\pi(\mathbf{x}_0) = \mathbb{E}_{\mathbf{x}} \left[\phi(\mathbf{x}_T) + \sum_{t=0}^{T-1} \ell(\mathbf{x}_t, \pi(\mathbf{x}_t)) \right], \quad (2)$$

where $\phi(\mathbf{x}_T)$ is the final cost, $\ell(\mathbf{x}_t, \pi(\mathbf{x}_t))$ is the instantaneous cost and $\mathbf{u}_t = \pi(\mathbf{x}_t, t)$ is a function that maps states and time to control. The cost $\mathcal{J}^\pi(\mathbf{x}_0)$ is defined as the expectation of the total cost accumulated from 0 to T .

B. Gaussian Process State-Space Model

The core idea of GPSSM is to model the transition model $f(\cdot)$ and/or measurement model $g(\cdot)$ using GPs, which are probability distributions over functions [14, 29]. A GP is specified completely by its mean function $m(\cdot)$ and covariance/kernel function $k(\cdot, \cdot)$ [30]. The covariance functions are the key ingredient in using GP, which encodes all assumptions about the form of function that we want to model. In general, the covariance function represents some form of distance or similarity. For a series of points $\mathbf{X} = [\mathbf{x}_i]_{i=1}^N$ in the domain of the function, any finite subset of function evaluations $\mathbf{f} = [f(\mathbf{x}_i)]_{i=1}^N$ are jointly Gaussian as given by:

$$p(\mathbf{f} | \mathbf{X}) = \mathcal{N}(\mathbf{f} | \mathbf{m}_{\mathbf{X}}, \mathbf{K}_{\mathbf{X}, \mathbf{X}}), \quad (3)$$

where $\mathbf{m} = [m(\mathbf{x}_i)]_{i=1}^N$ is the prior mean function and matrix $\mathbf{K}_{\mathbf{X}, \mathbf{X}}$ involves evaluations of the covariance

function at all pairs of data points in \mathbf{X} . Since the conditional distribution of a GP is another GP, the predictive distribution at a new input point \mathbf{x}^* is obtained by:

$$p(f^* | \mathbf{x}^*, \mathbf{f}, \mathbf{X}) = \mathcal{N}(f^* | \mu, \sigma^2), \quad (4)$$

with posterior mean and variance:

$$\begin{aligned} \mu &= m_{\mathbf{x}^*} + \mathbf{k}_{\mathbf{x}^*, \mathbf{X}} \mathbf{K}_{\mathbf{X}, \mathbf{X}}^{-1} (\mathbf{f} - \mathbf{m}_{\mathbf{X}}), \\ \sigma^2 &= k_{\mathbf{x}^*, \mathbf{x}^*} - \mathbf{k}_{\mathbf{x}^*, \mathbf{X}} \mathbf{K}_{\mathbf{X}, \mathbf{X}}^{-1} \mathbf{k}_{\mathbf{X}, \mathbf{x}^*}, \end{aligned} \quad (5)$$

where $k_{A,B}$ denotes the $|A| \times |B|$ matrix of the covariances evaluated at all pairs of A and B .

By employing independent GP priors on the transition model $f(\cdot)$ in (1) for each output dimension of \mathbf{x}_t , the transition model of GPSSM can be represented by:

$$p(\mathbf{x}_t | \mathbf{f}_t, \sigma_f^2 \mathbf{I}), \quad (6)$$

with

$$\begin{aligned} \mathbf{f}_t &= [f_d(\tilde{\mathbf{x}}_{t-1})]_{d=1}^D, \\ f_d(\tilde{\mathbf{x}}) &\sim \mathcal{GP}(m_d(\tilde{\mathbf{x}}), k_d(\tilde{\mathbf{x}}, \tilde{\mathbf{x}})), \end{aligned} \quad (7)$$

where the short-hand notation $\tilde{\mathbf{x}}_t = [\mathbf{x}_t, \mathbf{u}_t]$ denotes the input of the transition model at time t . In order to specify a GP, we need to define a mean function $m(\cdot)$ and a covariance function (also called kernel) $k(\cdot, \cdot)$. Generally, zero mean function is widely adopted. When a rough model of the dynamics is available it can be incorporated instead, which helps in obtaining meaningful distributions over the state trajectories from the first learning iterations. A common choice for a covariance function is the squared exponential kernel. Since we utilize the gradient-based inference scheme (cf. Section IV), any differentiable covariance function can be incorporated instead. Placing GP priors on both f and g can lead to *serious non-identifiability* problems [29]. To mitigate this, we assume a linear measurement mapping [4, 11]:

$$p(\mathbf{y}_t | \mathbf{x}_t) = \mathcal{N}(\mathbf{y}_t | g(\mathbf{x}_t), \sigma_g^2 \mathbf{I}) \quad (8)$$

where $g(\mathbf{x}_t) = \mathbf{C} \mathbf{x}_t$ and $\mathbf{C} = [\mathbf{I}, \mathbf{0}] \in \mathbb{R}^{O \times D}$ ($O \leq D$).

To alleviate the computational cost, the true GP predictive distribution is approximated with M pseudo inducing points $\boldsymbol{\eta}_d = [\eta_d^m]_{m=1}^M$ and corresponding inducing outputs $\mathbf{z}_d = [f_d(\boldsymbol{\eta}_d)]$ for each state dimension d . Pseudo inducing outputs are a subset of the function values $\mathbf{f} = \{\mathbf{f}^{\neq \mathbf{z}}, \mathbf{z}\}$, where $\mathbf{z} \equiv [\mathbf{z}_1, \dots, \mathbf{z}_D]$. Thus, the full joint distribution of the GPSSM can be represented by:

$$\begin{aligned} p(\mathbf{y}, \mathbf{x}, \mathbf{f}) &= p(\mathbf{x}, \mathbf{f}) p(\mathbf{y} | \mathbf{x}) \\ &= p(\mathbf{x}, \mathbf{f}^{\neq \mathbf{z}} | \mathbf{z}) p(\mathbf{z}) p(\mathbf{y} | \mathbf{x}), \end{aligned} \quad (9)$$

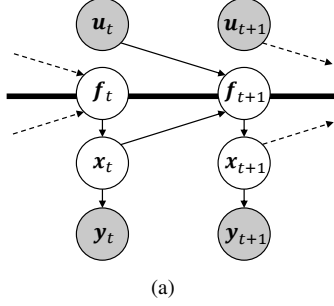


Fig. 1: Graphical model of GPSSM. White nodes and gray nodes represent latent and observed variables, respectively. The thick lines indicate sets of fully connected variables, which are jointly Gaussian under a GP prior.

where

$$\begin{aligned}
 p(\mathbf{x}, \mathbf{f}^{\neq \mathbf{z}} | \mathbf{z}) &= p(\mathbf{x}_0) \left[\prod_{t=1}^T p(\mathbf{x}_t | \mathbf{f}_t^{\neq \mathbf{z}}) \right] \\
 &\quad \left[\prod_{t=1}^T \prod_{d=1}^D p(f_{t,d}^{\neq \mathbf{z}_d} | \tilde{\mathbf{x}}_{t-1}, \mathbf{z}_d) \right], \\
 p(\mathbf{z}) &= \prod_{d=1}^D p(\mathbf{z}_d), \quad p(\mathbf{z}_d) = \mathcal{N}(\mathbf{z}_d | \mathbf{m}_{\eta_d}, \mathbf{K}_{\eta_d, \eta_d}), \\
 p(\mathbf{y} | \mathbf{x}) &= \prod_{t=0}^T p(\mathbf{y}_t | \mathbf{x}_t).
 \end{aligned} \tag{10}$$

IV. VARIATIONAL INFERENCE IN GPSSM

This section presents an inference method for learning the GPSSM. Learning the GPSSM is generally intractable due to the nonlinearity and non-Gaussianity of the dynamics model in a latent state. However, the log marginal likelihood $\log p(\mathbf{y})$ can be bounded to Evidence Lower Bound (ELBO) by using a variational inference scheme. In the following, we first define an approximation to true posterior of GPSSM based on the stochastic variational inference scheme [11,22] and derive ELBO via Jensen's inequality. We then present an online inference method of the GPSSM (onlineGPSSM) to efficiently handle sequentially arriving data¹. The onlineGPSSM follows a Bayesian approach, but employs online VI to approximate the intractable posterior distribution.

A. Stochastic Variational Inference

Following the stochastic variational inference scheme [11,22], we adopt a variational approximation to the true posterior distribution $p(\mathbf{x}, \mathbf{f} | \mathbf{y})$, which does not

¹In this paper, we use the terms 'data' and 'measurements' interchangeably.

assume factorisation between the latent functions $\mathbf{f}^{\neq \mathbf{z}}(\cdot)$ and the state trajectories \mathbf{x} but takes into account the true transition model based on the sparse GP approximation from (9). By employing a mean-field variational approximation to the posterior for \mathbf{z} , the inducing output distribution is given by $q(\mathbf{z}) = \prod_{d=1}^D \mathcal{N}(\mathbf{z}_d | \boldsymbol{\mu}_d, \boldsymbol{\Sigma}_d)$ for each latent state dimension d [31]. Integrating with respect to the inducing outputs, the predictive distribution of GP is obtained as Gaussian with a mean and variance given by:

$$\begin{aligned}
 \boldsymbol{\mu}_d &= m_{\tilde{\mathbf{x}}_t} + \mathbf{k}_{\tilde{\mathbf{x}}_t, \eta_d} \mathbf{K}_{\eta_d, \eta_d}^{-1} [\boldsymbol{\mu}_d - \mathbf{m}_{\eta_d}], \\
 \sigma_d^2 &= k_{\tilde{\mathbf{x}}_t, \tilde{\mathbf{x}}_t} - \alpha(\tilde{\mathbf{x}}_t) [\mathbf{K}_{\eta_d, \eta_d} - \boldsymbol{\Sigma}_d] \alpha(\tilde{\mathbf{x}}_t)^\top,
 \end{aligned} \tag{11}$$

where $\alpha(\tilde{\mathbf{x}}_t) = \mathbf{k}_{\tilde{\mathbf{x}}_t, \eta_d} \mathbf{K}_{\eta_d, \eta_d}^{-1}$.

With the approximate distribution for the variational posterior defined in (11), the variational distribution is given by:

$$\begin{aligned}
 q(\mathbf{x}, \mathbf{f}) &= p(\mathbf{x}, \mathbf{f}^{\neq \mathbf{z}} | \mathbf{z}) q(\mathbf{z}) q(\mathbf{x}_0) \\
 &= q(\mathbf{x}_0) \left[\prod_{t=1}^T p(\mathbf{x}_t | \mathbf{f}_t^{\neq \mathbf{z}}) \right] \left[\prod_{t=1}^T \prod_{d=1}^D p(f_{t,d}^{\neq \mathbf{z}_d} | \tilde{\mathbf{x}}_{t-1}, \mathbf{z}_d) q(\mathbf{z}_d) \right],
 \end{aligned} \tag{12}$$

where $q(\mathbf{x}_0) = \mathcal{N}(\mathbf{x}_0 | \boldsymbol{\mu}_{\mathbf{x}_0}, \boldsymbol{\Sigma}_{\mathbf{x}_0})$ and $q(\mathbf{z}_d) = \mathcal{N}(\mathbf{z}_d | \boldsymbol{\mu}_d, \boldsymbol{\Sigma}_d)$. The variational distribution in (12) is the optimal solution in sparse GP regression [31]. The number of hyper-parameters to be learned is proportional to the dimension of the latent dynamics regardless of the length of time, and is defined by initial state distribution, measurement model parameters that include measurement noise σ_g^2 , system noise, inducing points, inducing outputs and GP kernel parameters $\vartheta = (\boldsymbol{\mu}_{\mathbf{x}_0}, \boldsymbol{\Sigma}_{\mathbf{x}_0}, \theta_y, \sigma_{f,1:D}^2, \boldsymbol{\eta}_{1:D}, \boldsymbol{\mu}_{1:D}, \boldsymbol{\Sigma}_{1:D}, \theta_{1:D})$.

1) *Evidence Lower Bound (ELBO) and Stochastic ELBO evaluation:* Following standard variational inference methodology, the evidence lower bound (ELBO) is given by:

$$\begin{aligned}
 \log p(\mathbf{y} | \vartheta) &\geq \mathbb{E}_{q(\mathbf{x}, \mathbf{f} | \vartheta)} \left[\log \frac{p(\mathbf{y}, \mathbf{x}, \mathbf{f} | \vartheta)}{q(\mathbf{x}, \mathbf{f} | \vartheta)} \right] \\
 &= \log p(\mathbf{y} | \vartheta) - \mathcal{D}_{KL}(q(\mathbf{x}, \mathbf{f} | \vartheta) \| p(\mathbf{x}, \mathbf{f} | \mathbf{y}, \vartheta)).
 \end{aligned} \tag{13}$$

Solving this maximization problem is equivalent to finding the member of the family that is closest in KL divergence to the posterior. From equations (9) and (12), the ELBO can be transformed into:

$$\begin{aligned}
 \mathcal{L}(\vartheta) &= \sum_{t=0}^T \mathbb{E}_{q(\mathbf{x}_t)} [\log p(\mathbf{y}_t | \mathbf{x}_t)] \\
 &\quad - \mathcal{D}_{KL}(q(\mathbf{x}_0) \| p(\mathbf{x}_0)) - \sum_{d=1}^D \mathcal{D}_{KL}(q(\mathbf{z}_d) \| p(\mathbf{z}_d)).
 \end{aligned} \tag{14}$$

The first term encourages state trajectories that give high probability to the measured data. The second term encourages the state trajectory to start in a region of the state space where the prior is high. Here, we assume that a prior distribution of an initial latent state $p(\mathbf{x}_0)$ can be given. In many cases, the control/planning problems of a system are specified with some uncertain prior knowledge of the system's initial state given by the probability distribution $p(\mathbf{x}_0)$, which can be effectively used to learn the system model. In addition, the informative prior distribution of the initial state can be obtained by using Bayesian filtering and the system model learned previously via online learning (see Section IV-B and V). The last part of the ELBO regularizes the approximate posterior to remain close to the GP prior. A full derivation is provided in Appendix A. For a more detailed explanation, we refer readers to [11,22] and the references therein.

We can now learn the GPSSM by maximizing the ELBO with respect to the hyper-parameters ϑ . The second and third terms of the ELBO can be computed analytically because they are a KL-divergence between the two Gaussian distributions. However, the first term requires an expectation for latent state distribution $q(\mathbf{x})$ and its analytic evaluation is intractable. The Markovian structure of the latent states and the sparse GP approximation can be used to enable a differentiable sampling-based estimation of the expectation term [11]. Samples $\tilde{\mathbf{x}}_t \sim q(\mathbf{x}_t)$ are recursively obtained for time $t = 1, \dots, T$ by drawing from the sparse GP posterior in (11). The distribution of the current latent state $q(\mathbf{x}_t)$ is independent of past time steps, given the latent state distribution $q(\mathbf{x}_{t-1})$ at the previous time step and the explicit representation of GP inducing points. By using the reparametrisation trick [25], drawing samples can be differentiable for the hyper-parameters Θ , which draw samples $\varepsilon \sim \mathcal{N}(0, 1)$ and then compute the following equation:

$$\hat{\mathbf{x}}_{t+1,d} = \mu_d(\tilde{\mathbf{x}}_t) + \varepsilon \sqrt{\sigma_d^2(\tilde{\mathbf{x}}_t, \tilde{\mathbf{x}}_t) + \sigma_{f,d}^2}, \quad (15)$$

where $\tilde{\mathbf{x}}_t = (\hat{\mathbf{x}}_t, \mathbf{u}_t)$ and $\hat{\mathbf{x}}_0 \sim q(\mathbf{x}_0)$. Due to the reparametrisation trick, the gradient can be propagated back through time. From (15), an unbiased estimator of the first term in the ELBO is represented by:

$$\mathbb{E}_{q(\mathbf{x}_t)} [\log p(\mathbf{y}_t | \mathbf{x}_t)] \approx \frac{1}{N} \sum_{i=1}^N \log p(\mathbf{y}_t | \hat{\mathbf{x}}_t^{(i)}). \quad (16)$$

B. Online Variational Inference

In most dynamical systems, measurement arrives in a sequential manner and the new measurement \mathbf{y}' is added to old measurements \mathbf{y} . Storing all the data requires large memory, and using it for model learning can be computationally infeasible. Specifically, storage demand

and computational complexity increase in proportion to the amount data, which is time T (The complexity is $\mathcal{O}(TM^2)$ and the storage is $\mathcal{O}(TM)$ for each sample trajectory). Furthermore, when systems or environments change, using all of the previous data for system model learning makes it difficult to identify the changed system. Thus, the goal of online learning is to learn a system model that can be used for anytime prediction and control, and the system model should be able to adapt to changes in the system or environment without forgetting the knowledge from the previous data.

Following a Bayesian approach, we assume that only the current measurements \mathbf{y}' is directly accessible and the information from the previous measurements \mathbf{y} is implied in the approximate posterior of the latent dynamics learned in the previous step. The effect of the old measurements \mathbf{y} on current approximate posterior $q(\cdot | \vartheta')$ is induced to propagate through previous approximate posterior $q(\cdot | \vartheta)$. Based on (13), an approximation to the true posterior at the previous step is represented as $q(\mathbf{x}, \mathbf{f} | \vartheta)$, which must be propagated to form the new approximation $q(\mathbf{x}, \mathbf{f} | \vartheta')$.

$$\begin{aligned} q(\mathbf{x}, \mathbf{f} | \vartheta) &\approx p(\mathbf{x}, \mathbf{f} | \mathbf{y}, \vartheta) \\ &= \frac{1}{p(\mathbf{y} | \vartheta)} p(\mathbf{x}, \mathbf{f} | \vartheta) p(\mathbf{y} | \mathbf{x}), \end{aligned} \quad (20)$$

$$\begin{aligned} q(\mathbf{x}, \mathbf{f} | \vartheta') &\approx p(\mathbf{x}, \mathbf{f} | \mathbf{y}, \mathbf{y}', \vartheta') \\ &= \frac{1}{p(\mathbf{y}, \mathbf{y}' | \vartheta')} p(\mathbf{x}, \mathbf{f} | \vartheta') p(\mathbf{y} | \mathbf{x}) p(\mathbf{y}' | \mathbf{x}). \end{aligned} \quad (21)$$

To update the true posterior $p(\mathbf{x}, \mathbf{f} | \mathbf{y}, \mathbf{y}', \vartheta')$, we use an approximation of $p(\mathbf{y} | \mathbf{x})$ by inverting (20), that is $p(\mathbf{y} | \mathbf{x}) \approx p(\mathbf{y} | \vartheta) q(\mathbf{x}, \mathbf{f} | \vartheta) / p(\mathbf{x}, \mathbf{f} | \vartheta)$. By doing this, (21) is transformed into:

$$\begin{aligned} \hat{p}(\mathbf{x}, \mathbf{f} | \mathbf{y}, \mathbf{y}', \vartheta') &= \\ &\frac{p(\mathbf{y} | \vartheta)}{p(\mathbf{y}, \mathbf{y}' | \vartheta')} p(\mathbf{x}, \mathbf{f} | \vartheta') p(\mathbf{y}' | \mathbf{x}) \frac{q(\mathbf{x}, \mathbf{f} | \vartheta)}{p(\mathbf{x}, \mathbf{f} | \vartheta)}. \end{aligned} \quad (22)$$

Although it appears to be available as a new posterior $q(\mathbf{x}, \mathbf{f} | \vartheta')$, this reverts to the problem of learning the exact GPSSM for new measurements with fixed hyperparameters and it is intractable. Thus, we consider a variational update that employs a projection operator defined through KL minimization, which converts the distribution to a tractable form using new hyperparameters similar to the variational update in GP [27]. We allow the locations of inducing points in the new approximation to be different from those in the old one. Let $\mathbf{a} = f(\boldsymbol{\eta})$ and $\mathbf{b} = f(\boldsymbol{\eta}')$ be the function values at the inducing points before and after obtaining new measurements. The previous approximate posterior is given by $q(\mathbf{x}, \mathbf{f} | \vartheta) = p(\mathbf{x}, \mathbf{f}^{\neq \mathbf{a}} | \mathbf{a}, \theta) q(\mathbf{a}) q(\mathbf{x}_0)$, where $q(\mathbf{a}) = \mathcal{N}(\mathbf{a}; \boldsymbol{\mu}_a, \boldsymbol{\Sigma}_a)$ and $q(\mathbf{x}_0) = \mathcal{N}(\mathbf{x}_0; \boldsymbol{\mu}_{x_0}, \boldsymbol{\Sigma}_{x_0})$.

$$\begin{aligned} \mathcal{D}_{KL}(q(\mathbf{x}, \mathbf{f} \mid \vartheta') \parallel \hat{p}(\mathbf{x}, \mathbf{f} \mid \mathbf{y}, \mathbf{y}', \vartheta')) &= \mathbb{E}_{q(\mathbf{x}, \mathbf{f} \mid \vartheta')} \left[\log \frac{q(\mathbf{x}, \mathbf{f} \mid \vartheta')}{\frac{p(\mathbf{y} \mid \vartheta')}{p(\mathbf{y}, \mathbf{y}' \mid \vartheta')} p(\mathbf{x}, \mathbf{f} \mid \vartheta') p(\mathbf{y}' \mid \mathbf{x}) \frac{q(\mathbf{x}, \mathbf{f} \mid \vartheta')}{p(\mathbf{x}, \mathbf{f} \mid \vartheta')}} \right] \\ &= \log \frac{p(\mathbf{y}, \mathbf{y}' \mid \vartheta')}{p(\mathbf{y} \mid \vartheta')} + \mathbb{E}_{q(\mathbf{x}, \mathbf{f} \mid \vartheta')} \left[\log \frac{q'(\mathbf{b})q(\mathbf{x}'_0)}{p(\mathbf{b} \mid \theta')p(\mathbf{x}'_0)p(\mathbf{y}' \mid \mathbf{x}) \frac{q(\mathbf{a})q(\mathbf{x}_0)}{p(\mathbf{a} \mid \theta)p(\mathbf{x}_0)}} \right] \end{aligned} \quad (17)$$

$$\begin{aligned} \mathcal{NL}(\vartheta') &= - \sum_{t=0}^T \mathbb{E}_{q(\mathbf{x}_t)} [\log p(\mathbf{y}_t \mid \mathbf{x}_t)] + \mathcal{D}_{KL}(q(\mathbf{x}'_0) \parallel p(\mathbf{x}'_0)) + \sum_{d=1}^D \mathcal{D}_{KL}(q'(\mathbf{b}_d) \parallel p(\mathbf{b}_d \mid \theta'_d)) \\ &\quad + \sum_{d=1}^D \mathcal{D}_{KL}(q'(\mathbf{a}_d) \parallel q(\mathbf{a}_d)) - \sum_{d=1}^D \mathcal{D}_{KL}(q'(\mathbf{a}_d) \parallel p(\mathbf{a}_d \mid \theta_d)) \end{aligned} \quad (18)$$

$$\begin{aligned} q'(\mathbf{a}_d) &= \int p(\mathbf{a}_d \mid \mathbf{b}_d, \theta'_d) q'(\mathbf{b}_d) d\mathbf{b}_d \\ &= \mathcal{N}(\mathbf{a}_d; \mathbf{m}_{\eta_d} + \mathbf{K}_{\eta_d \eta'_d} \mathbf{K}_{\eta'_d \eta'_d}^{-1} [\boldsymbol{\mu}_{\mathbf{b}, d} - \mathbf{m}_{\eta'_d}], \mathbf{S}_{\mathbf{a}_d | \mathbf{b}_d} + \mathbf{K}_{\eta_d \eta'_d} \mathbf{K}_{\eta'_d \eta'_d}^{-1} \boldsymbol{\Sigma}_{\mathbf{b}, d} \mathbf{K}_{\eta'_d \eta'_d}^{-1} \mathbf{K}_{\eta'_d \eta_d}) \\ \mathbf{S}_{\mathbf{a}_d | \mathbf{b}_d} &= \mathbf{K}_{\eta_d \eta_d} - \mathbf{K}_{\eta_d \eta'_d} \mathbf{K}_{\eta'_d \eta'_d}^{-1} \mathbf{K}_{\eta'_d \eta_d} \end{aligned} \quad (19)$$

The new posterior approximation is also represented in the same form, but with the new hyperparameters, $q(\mathbf{x}, \mathbf{f} \mid \vartheta') = p(\mathbf{x}, \mathbf{f}^{\neq \mathbf{b}} \mid \mathbf{b}, \theta') q'(\mathbf{b}) q(\mathbf{x}'_0)$ where $q'(\mathbf{b}) = \mathcal{N}(\mathbf{b}; \boldsymbol{\mu}_{\mathbf{b}}, \boldsymbol{\Sigma}_{\mathbf{b}})$ and $q(\mathbf{x}'_0) = \mathcal{N}(\mathbf{x}'_0; \boldsymbol{\mu}_{\mathbf{x}'_0}, \boldsymbol{\Sigma}_{\mathbf{x}'_0})$. This approximate inference problem can be transformed into an optimization problem that minimizes the KL divergence using the variational inference as shown in (17).

Since the KL divergence is non-negative, the second term in (17) is the negative approximate lower bound of the log marginal likelihood represented as $\log p(\mathbf{y}, \mathbf{y}' \mid \vartheta') / p(\mathbf{y} \mid \vartheta) \approx p(\mathbf{y}' \mid \mathbf{y})$. The negative lower bound is derived in the same way as the equations (13) and (14), but slightly different in that it includes $q(\mathbf{x}, \mathbf{f} \mid \vartheta) / p(\mathbf{x}, \mathbf{f} \mid \vartheta) = q(\mathbf{a})q(\mathbf{x}_0) / p(\mathbf{a} \mid \theta)p(\mathbf{x}_0)$. The term related to \mathbf{x}_0 serves to propagate the effect of the previous initial state \mathbf{x}_0 to the current initial state \mathbf{x}'_0 . This term can be neglected if the initial state is sufficiently broad. Thus, the negative evidence lower bound (negative ELBO) of the approximate online log marginal likelihood is represented by (18). The first three terms form the variational bound given if the new measurements are the whole of the training data, and the last two terms lead the posterior to take into account the old likelihood through the approximate posterior and the prior. See Appendix B for details about the derivation of (18). For fixed hyperparameters (i.e., the positions of inducing inputs and kernel parameters), the online variational inference is equivalent to the vanilla application of streaming variational Bayes (streaming-

VB) [21] to the GPSSM setting in which the previous posterior plays the role of an new prior for the new measurements [14].

V. ONLINE LEARNING AND PLANNING

In this section, we introduce our online learning and planning framework (i.e., reinforcement learning) that employs a combination of probabilistic inference, Bayesian filtering and trajectory optimization.

A. Multi-Step Prediction and Bayesian Filtering

Multi-step predictions for a given initial state and control inputs are essential to solve the control/planning problem described in (2). Let $p(\mathbf{x}_t, \mathbf{u}_t) = p(\tilde{\mathbf{x}}_t) \sim \mathcal{N}(\tilde{\boldsymbol{\mu}}_t, \tilde{\mathbf{P}}_t)$ be the joint distribution over the state-control pair at t . Then the distribution over the state transition becomes $p(\mathbf{x}_{t+1}) = \int p(f(\tilde{\mathbf{x}}_t) \mid \tilde{\mathbf{x}}_t) p(\tilde{\mathbf{x}}_t) d\tilde{\mathbf{x}}_t$. Generally, this predictive distribution leads to a non-Gaussian predictive distribution. However, the predictive distribution can be approximated by a Gaussian using moment matching [9,32] or the linearization approach [5,33]. In this work, we employ the linearization approach. Since taking a derivative is a linear operation, the derivative of a GP is another GP [33]. Thus the state distribution at $t+1$ is represented by a Gaussian $p(\mathbf{x}_{t+1}) \sim \mathcal{N}(\boldsymbol{\mu}_{t+1}, \mathbf{P}_{t+1})$. The predicted mean $\boldsymbol{\mu}_{t+1}$ is obtained by evaluating the posterior GP mean in (11) at the mean $\tilde{\boldsymbol{\mu}}_t$ of the input distribution $p(\tilde{\mathbf{x}}_t)$. To compute the GP predictive covariance \mathbf{P}_{t+1} , we explicitly linearize the posterior GP mean function around $\tilde{\boldsymbol{\mu}}_t$ and denote it as

A_t . By employing a bayesian filtering framework [5], the predictive covariance is given by:

$$P_{t+1} = (I - K_t H_t) \bar{P}_t, \quad (23)$$

with

$$\begin{aligned} \bar{P}_{t+1} &= A_t P_t A_t^\top + \Sigma_{s,t}, \\ K_t &= \bar{P}_{t+1} H_t^\top (H_t \bar{P}_{t+1} H_t^\top + \Sigma_g)^{-1}, \\ H_t &= \left. \frac{\partial g(\tilde{x}_t)}{\partial \tilde{x}_t} \right|_{\mu_t, u_t}. \end{aligned} \quad (24)$$

In (23), $\Sigma_{s,t}$ is a diagonal matrix whose entries are the sum of the system noise variances $\sigma_{f,d}^2$ and the latent dynamics uncertainties σ_d^2 evaluated at $\tilde{\mu}_t$ as in (11). Σ_g is the measurement noise variance σ_g^2 . K_t is often called Kalman gain [34]. Given a measurements y_t , an estimate of the state $\hat{\mu}_t$ is obtained by:

$$\hat{\mu}_t = \mu_t + K_t [y_t - g(\tilde{x}_t)] \quad (25)$$

B. Probabilistic Trajectory Optimization

Based on multi-step predictions, we now consider the control/planning problem (2) for the learned system model. In order to incorporate model uncertainty explicitly, we adopt belief space iterative Linear Quadratic Gaussian (belief space iLQG [28]) and perform trajectory optimization in the belief space. The belief space iLQG extends the iLQG method [35] to Partially Observable Markov Decision Processes (POMDPs) by using a Gaussian belief instead of the fully observable state, which employs a standard extended Kalman filter (EKF) to represent belief dynamics. Accordingly, the belief space iLQG finds a locally optimal trajectory for known belief dynamics and cost function using an iterative procedure. It proceeds by, first, linearizing belief dynamics forward in time around the nominal trajectory for which a locally optimal control law can then be computed backwards in time. These steps are repeated until convergence to the locally optimal trajectory.

1) *Approximate Belief Dynamics and Cost Function:* The belief space iLQG assumes a dynamics model is given and the stochasticity comes from the process and sensor noises, but we use the learned dynamics model and nominal trajectory distribution that is a state distribution-control pair $(p(\tilde{x}_t), \bar{u}_t)$. To incorporate uncertainty explicitly into the local model, we define the belief state as $\mathbf{b}_t = [\mu_t, \text{vec}(P_t)]^\top \in \mathcal{R}^{D+D(D+1)/2}$ (P_t is symmetric) where $\text{vec}(\cdot)$ denotes the vectorization. Based on equations (11) and (23), the belief dynamics with the augmented state \mathbf{b}_t is given by:

$$\mathbf{b}_{t+1} = \mathcal{F}(\mathbf{b}_t, \mathbf{u}_t). \quad (26)$$

Based on the belief dynamics, the original cost function (2) is reformulated by:

$$\mathcal{J}^\pi(\mathbf{b}_0) = \phi(\mathbf{b}_T) + \sum_{t=0}^{T-1} \ell(\mathbf{b}_t, \mathbf{u}_t), \quad (27)$$

where

$$\begin{aligned} \phi(\mathbf{b}_T) &= \mathbb{E}[\phi(\mathbf{x}_T)] \\ &= \text{tr}(Q_T P_T) + (\mu_T - \mathbf{x}_{goal})^\top \tilde{Q}_T (\mu_T - \mathbf{x}_{goal}), \\ \ell(\mathbf{b}_t, \mathbf{u}_t) &= \mathbb{E}[\ell(\mathbf{x}_t, \pi(\mathbf{x}_t))] \\ &= \text{tr}(Q P_t) + \mathbf{u}_t^\top R \mathbf{u}_t + \alpha(\mu_t), \end{aligned} \quad (28)$$

for a given $Q_t \geq 0$ and $R_t > 0$. The term $\text{tr}(Q_T P_T) + (\mu_T - \mathbf{x}_{goal})^\top \tilde{Q}_T (\mu_T - \mathbf{x}_{goal})$ encodes the final cost of arriving at the goal \mathbf{x}_{goal} , $\mathbf{u}_t^\top R_t \mathbf{u}_t$ penalizes the control effort along the trajectory, $\text{tr}(Q_t P_t)$ penalizes the uncertainty, and $\alpha(\mu_t)$ encodes the state constraints (e.g., motion and collision).

2) *Control Policy:* By linearizing the belief dynamics around the nominal trajectory distribution, the approximate dynamics are expressed as:

$$\begin{aligned} \mathbf{b}_{t+1} - \bar{\mathbf{b}}_{t+1} &\approx \mathcal{F}_{b,t}(\mathbf{b}_t - \bar{\mathbf{b}}_t) + \mathcal{F}_{u,t}(\mathbf{u}_t - \bar{\mathbf{u}}_t), \\ W_{(i)}(\mathbf{b}_t, \mathbf{u}_t) &\approx \mathbf{e}_t^i + \mathcal{F}_{b,t}^{(i)}(\mathbf{b}_t - \bar{\mathbf{b}}_t) + \mathcal{F}_{u,t}^{(i)}(\mathbf{u}_t - \bar{\mathbf{u}}_t), \end{aligned} \quad (29)$$

where

$$\begin{aligned} \mathcal{F}_{b,t} &= \frac{\partial \mathcal{F}}{\partial \mathbf{b}}(\bar{\mathbf{b}}_t, \bar{\mathbf{u}}_t), \quad \mathcal{F}_{u,t} = \frac{\partial \mathcal{F}}{\partial \mathbf{u}}(\bar{\mathbf{b}}_t, \bar{\mathbf{u}}_t), \\ \mathbf{e}_t^i &= W_{(i)}(\bar{\mathbf{b}}_t, \bar{\mathbf{u}}_t), \quad \mathcal{F}_{b,t}^i = \frac{\partial W_{(i)}}{\partial \mathbf{b}}(\bar{\mathbf{b}}_t, \bar{\mathbf{u}}_t), \\ \mathcal{F}_{u,t}^i &= \frac{\partial W_{(i)}}{\partial \mathbf{u}}(\bar{\mathbf{b}}_t, \bar{\mathbf{u}}_t). \end{aligned}$$

$W_{(i)}(\mathbf{b}_t, \mathbf{u}_t)$ is the i -th column of matrix $W(\mathbf{b}_t, \mathbf{u}_t)$. Note that $W_{(i)}(\mathbf{b}_t, \mathbf{u}_t)$ has n columns, where n is the dimension of the state. For a general nonquadratic cost function, we approximate it as a quadratic function along the nominal belief and control trajectory $(\bar{\mathbf{b}}, \bar{\mathbf{u}})$,

$$\begin{aligned} \ell(\mathbf{b}_t, \mathbf{u}_t) &\approx \frac{1}{2} \begin{bmatrix} \delta \mathbf{b}_t \\ \delta \mathbf{u}_t \end{bmatrix}^\top \begin{bmatrix} \ell_{bb,t} & \ell_{bu,t} \\ \ell_{ub,t} & \ell_{uu,t} \end{bmatrix} \begin{bmatrix} \delta \mathbf{b}_t \\ \delta \mathbf{u}_t \end{bmatrix} \\ &\quad + \begin{bmatrix} \delta \mathbf{b}_t \\ \delta \mathbf{u}_t \end{bmatrix}^\top \begin{bmatrix} \ell_{b,t} \\ \ell_{u,t} \end{bmatrix} + \ell_{0,t}, \end{aligned} \quad (30)$$

where $\ell_{0,t} = \ell(\bar{\mathbf{b}}_t, \bar{\mathbf{u}}_t)$. $\delta \mathbf{b}_t = \mathbf{b}_t - \bar{\mathbf{b}}_t$, $\delta \mathbf{u}_t = \mathbf{u}_t - \bar{\mathbf{u}}_t$ are deviations from the nominal trajectory and the terms with subscripts denote Jacobian and Hessian matrices of their respective functions.

Given the linear dynamics (29) and quadratic cost (30), we can obtain a quadratic approximation of the value function along the nominal trajectory $\bar{\mathbf{b}}_t$:

$$\mathbf{V}_t(\mathbf{b}_t) \approx \frac{1}{2} \delta \mathbf{b}_t^\top \mathbf{V}_{bb,t} \delta \mathbf{b}_t + \delta \mathbf{b}_t^\top \mathbf{V}_{b,t} + \mathbf{V}_{0,t}. \quad (31)$$

Following the dynamic programming principle [36], the Bellman equation for the value function $V_t(\mathbf{b}_t)$ and control policy $\pi_t(\mathbf{b}_t)$ in discrete-time are specified as:

$$\begin{aligned} V_t(\mathbf{b}_t) &= \min_{\mathbf{u}_t} \left(\ell(\mathbf{b}_t, \mathbf{u}_t) + \mathbb{E}[V_{t+1}(\mathcal{F}(\mathbf{b}_t, \mathbf{u}_t) + \mathbf{w}_t)] \right) \\ &= \min_{\mathbf{u}_t} \left(\ell(\mathbf{b}_t, \mathbf{u}_t) + \frac{1}{2} \delta \mathbf{b}_{t+1}^\top \mathbf{V}_{bb,t+1} \delta \mathbf{b}_{t+1} \right. \\ &\quad \left. + \delta \mathbf{b}_{t+1}^\top \mathbf{V}_{b,t+1} + \mathbf{V}_{0,t+1} \right. \\ &\quad \left. + \frac{1}{2} \text{tr}[W(\mathbf{b}_t, \mathbf{u}_t)^\top \mathbf{V}_{bb,t+1} W(\mathbf{b}_t, \mathbf{u}_t)] \right) \\ &= \min_{\mathbf{u}_t} Q(\mathbf{b}_t, \mathbf{u}_t), \\ \pi_t(\mathbf{b}_t) &= \underset{\mathbf{u}_t}{\text{argmin}} \left(\ell(\mathbf{b}_t, \mathbf{u}_t) + \mathbb{E}[V_{t+1}(\mathcal{F}(\mathbf{b}_t, \mathbf{u}_t) + \mathbf{w}_t)] \right), \end{aligned} \quad (32)$$

where

$$\text{tr}[W(\mathbf{b}_t, \mathbf{u}_t)^\top \mathbf{V}_{bb,t+1} W(\mathbf{b}_t, \mathbf{u}_t)] = \sum_{i=1}^m W_{(i)}(\mathbf{b}_t, \mathbf{u}_t).$$

By substituting equations (29) and (30) into (32), the Q-function is given by:

$$\begin{aligned} Q_t(\bar{\mathbf{b}}_t + \delta \mathbf{b}_t, \bar{\mathbf{u}}_t + \delta \mathbf{u}_t) &= \frac{1}{2} \begin{bmatrix} \delta \mathbf{b}_t \\ \delta \mathbf{u}_t \end{bmatrix}^\top \begin{bmatrix} Q_{bb,t} & Q_{bu,t} \\ Q_{ub,t} & Q_{uu,t} \end{bmatrix} \begin{bmatrix} \delta \mathbf{b}_t \\ \delta \mathbf{u}_t \end{bmatrix} \\ &\quad + \begin{bmatrix} \delta \mathbf{b}_t \\ \delta \mathbf{u}_t \end{bmatrix}^\top \begin{bmatrix} Q_{b,t} \\ Q_{u,t} \end{bmatrix} + Q_{0,t}, \end{aligned} \quad (33)$$

where

$$\begin{aligned} Q_{bb,t} &= \ell_{bb,t} + \mathcal{F}_{b,t}^\top \mathbf{V}_{bb,t+1} \mathcal{F}_{b,t} + \sum_{i=1}^m \mathcal{F}_{b,t}^{i\top} \mathbf{V}_{bb,t+1} \mathcal{F}_{b,t}^i, \\ Q_{b,t} &= \ell_{b,t} + \mathcal{F}_{b,t}^\top \mathbf{V}_{b,t+1} + \sum_{i=1}^m \mathcal{F}_{b,t}^{i\top} \mathbf{V}_{bb,t+1} \mathbf{e}_t^i, \\ Q_{uu,t} &= \ell_{uu,t} + \mathcal{F}_{u,t}^\top \mathbf{V}_{bb,t+1} \mathcal{F}_{u,t} + \sum_{i=1}^m \mathcal{F}_{u,t}^{i\top} \mathbf{V}_{bb,t+1} \mathcal{F}_{u,t}^i, \\ Q_{u,t} &= \ell_{u,t} + \mathcal{F}_{u,t}^\top \mathbf{V}_{b,t+1} + \sum_{i=1}^m \mathcal{F}_{u,t}^{i\top} \mathbf{V}_{bb,t+1} \mathbf{e}_t^i, \\ Q_{ub,t} &= \ell_{ub,t} + \mathcal{F}_{u,t}^\top \mathbf{V}_{bb,t+1} \mathcal{F}_{b,t} + \sum_{i=1}^m \mathcal{F}_{u,t}^{i\top} \mathbf{V}_{bb,t+1} \mathcal{F}_{b,t}^i, \\ Q_{0,t} &= \ell_{0,t} + \mathbf{V}_{0,t+1} + \sum_{i=1}^n \mathbf{e}_t^{i\top} \mathbf{V}_{bb,t+1} \mathbf{e}_t^i. \end{aligned} \quad (34)$$

In order to find the optimal control policy, we compute the local variations in control $\delta \hat{\mathbf{u}}$ that minimize the quadratic approximation of the Q-function in (32):

$$\begin{aligned} \delta \mathbf{u}_t^* &= \underset{\delta \mathbf{u}_t}{\text{argmax}} [Q_t(\bar{\mathbf{b}}_t + \delta \mathbf{b}_t, \bar{\mathbf{u}}_t + \delta \mathbf{u}_t)] \\ &= -\mathbf{Q}_{uu,t}^{-1} \mathbf{Q}_{u,t} - \mathbf{Q}_{uu,t}^{-1} \mathbf{Q}_{ub,t} \delta \mathbf{b}_t. \end{aligned} \quad (35)$$

The optimal control can be found as $\mathbf{u}_t^* = \bar{\mathbf{u}}_t + \delta \mathbf{u}_t^*$. Substituting (35) into (32) gives the value function

Algorithm 1 Online Learning and Planning

- 1: **Input:** Set control horizon T_c , planning horizon T_p , memory size \mathcal{M} .
 - 2: **Initialization:** Set $t = 0$, and the prior distribution of the initial state as $p(\mathbf{x}_0)$.
 - 3: **Model learning:** Learn GPSSM hyperparameters ϑ by maximizing the ELBO (14) based on prior knowledge or given measurements. \triangleright Section IV-A
 - 4: **Trajectory optimization:** Generate optimal control policy in the belief space based on the learned model and obtain $\mathbf{u}_{t:t+T_p-1}^*$. \triangleright Section V-B
 - 5: **repeat** \triangleright Main reinforcement learning loop
 - 6: **Interaction:** Apply the optimal control policy $\mathbf{u}_{t:t+T_c}^*$ to the system. Estimate $p(\mathbf{x}_t)$ using the measurements and learned model. Store the measurements and some state estimation results in memory. Update $t = t + T_c$. \triangleright Section V-A
 - 7: **Model adaptation:** Learn GPSSM hyperparameters ϑ' by minimizing the negative ELBO (18) based on the measurements and estimation results in memory. Update $\vartheta = \vartheta'$. \triangleright Section IV-B
 - 8: **Trajectory optimization:** Initialize with the previously optimized trajectory and generate a new optimal control policy $\mathbf{u}_{t:t+T_p-1}^*$ using the learned model specified as ϑ . \triangleright Section V-B
 - 9: **until** Operation time remained
-

$V_t(\mathbf{b}_t)$ as a function of only \mathbf{b}_t in the form of (31):

$$\begin{aligned} V_{bb,t} &= Q_{bb,t} - \mathbf{Q}_{ub,t}^\top \mathbf{Q}_{uu,t}^{-1} \mathbf{Q}_{ub,t}, \\ V_{b,t} &= Q_{b,t} - \mathbf{Q}_{ub,t}^\top \mathbf{Q}_{uu,t}^{-1} \mathbf{Q}_{u,t}, \\ V_{0,t} &= Q_{0,t} - \mathbf{Q}_{u,t}^\top \mathbf{Q}_{uu,t}^{-1} \mathbf{Q}_{u,t}. \end{aligned} \quad (36)$$

This recursion continues by computing a control policy for time step $t - 1$.

C. Summary of Algorithm

The proposed online learning and planning framework can be summarized in Algorithm 1. Here, the receding horizon scheme (RHC) is adopted. RHC, also known as model predictive control (MPC), is a form of feedback (i.e., closed-loop) control system. Our algorithm consists of offline (line 1-4) and online (line 5-9) parts. In the offline part, we first set the parameters needed for learning and planning. For given data or prior knowledge of the system, we optimize GPSSM hyperparameters by maximizing the ELBO. If an approximate model of the system is given, it can be used as a mean prior of the GPSSM to improve training time. We then perform trajectory optimization for the future time step T_p based on the learned model and obtain the optimal control policy $\mathbf{u}_{t:t+T_p-1}^*$.

Given a solution to a T_p -step trajectory optimization problem starting at $p(\mathbf{x}_0)$, we only apply a forepart

of T_p -step control input commands. We denote the length of the subset as control horizon T_c , which is determined by the available computational resources required for trajectory optimization ($T_c \leq T_p$). Measurements obtained from the sensor while interacting with the real environment are used to estimate the current state $p(x_t)$. Some state estimation results and measurements are stored in the memory, where old measurements are removed from the training set to keep memory size \mathcal{M} fixed. Specifically, instead of storing the state estimation results of every time step, we store the results of the uniform time interval set for the mini-batch training. The stored results are used as the prior distribution of the initial state for the online learning of the GPSSM. Online learning can be performed concurrently with other procedures, and the updated model is used again for trajectory planning. We initialize with the previous optimized trajectory. The T_p -step nominal control sequence for warm-start becomes $u_{t+T_c+1}^*, u_{t+T_c+2}^*, \dots, u_{t+T_p-1}^*, u_{t+T_p-1}^*$. This online trajectory optimization converges much faster than the offline case unless the task is too different from the previous one due to a warm-start. Our online learning and planning scheme is particularly suitable for applications with task, environment or model variations.

VI. NUMERICAL SIMULATIONS

In the following, we evaluate the onlineGPSSM and GPSSM-based RL framework using two simulated examples: a toy and thereafter the loitering task of a fixed-wing Unmanned Aerial Vehicle (UAV) in a wind field. In all the experiments, the squared exponential kernel with ARD length-scales is used, but any differentiable kernel can be incorporated. For the sparse approximation of the latent transition model represented by the GP, we used 20 pseudo inducing points for each output dimension of x_t . The onlineGPSSM, however, allows variations of the number of pseudo inducing points at each online learning step. Specifically, pseudo inducing points can be added.

A. A simple linear system

Although GPSSM is particularly suited to nonlinear system identification, we will start by illustrating the online learning approach with a simple linear system:

$$\begin{aligned} x_{t+1} &= 0.8x_t + u_t + w_f \\ y_t &= x_t + w_g \end{aligned} \quad (37)$$

with parameters $w_f = 0.1$, $w_g = 1$ and a known control input u_t . The measurement was generated by setting the control input to -2 for the first 30 seconds and then to 3 for 30 seconds. The online learning was performed in three steps at 20 second intervals. The state distribution

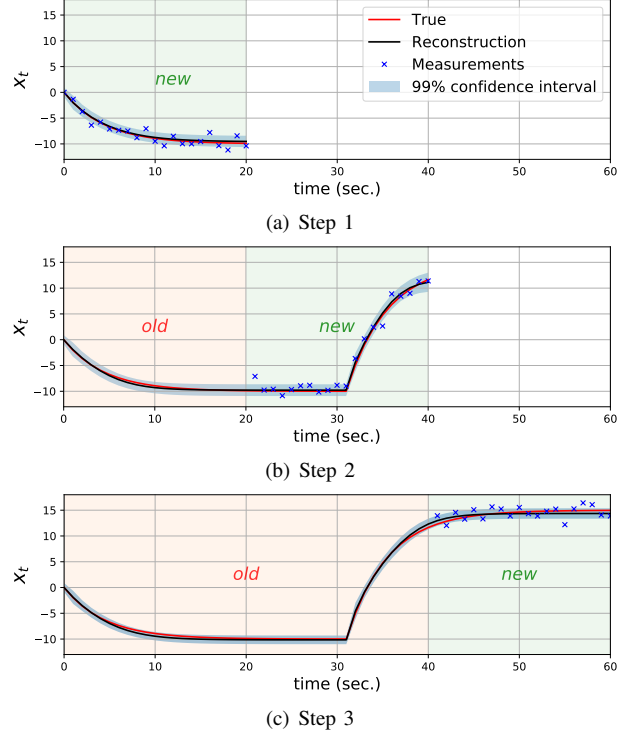


Fig. 2: Reconstruction results after each online learning.

at $t = 0$ is known, and the prior distribution of initial state for each online learning step is obtained through Bayesian filtering using the previously learned system model.

To verify the performance of onlineGPSSM, we reconstructed the state trajectory from the initial state x_0 using the learned system model and the known control inputs after each step of online learning. The reconstruction results are shown in Fig. 2. Each result indicates that the proposed method can reconstruct the past learning results well, even if it only uses recent measurements for system model learning. Figure 3 shows the prediction results of the mean and covariance after each step of online learning. As the results show, the hyperparameters of the GPSSM are automatically optimized to generate new measurements without forgetting the learned system knowledge from past measurements due to the last two terms of (18). Since the zero mean function was used in this experiment, the mean is zero for unexperienced areas. Also, the learned system model is not overconfident in regions of the space where data is scarce.

B. Loitering of fixed-wing UAV in a wind field

In this example, the proposed online learning and planning framework introduced in Section V is validated. We consider a circular loitering task of a fixed-wing UAV. Such a task is required for precise commu-

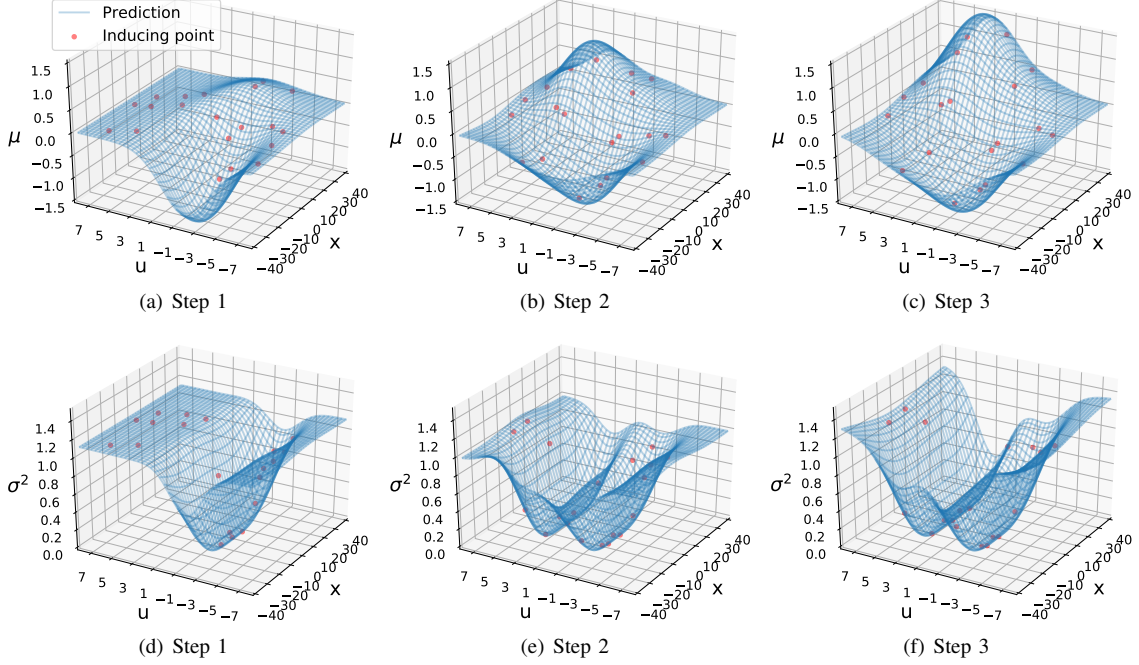


Fig. 3: The prediction results after each online learning: (a)-(c) mean and (d)-(f) covariance.

nication relay [37] as well as persistent monitoring [38] of specific areas. The true dynamics is given by [39,40]:

$$\begin{aligned}
 x_{1,t+1} &= x_{1,t} + (V \cos x_{3,t} + W_1(x_{1,t}, x_{2,t}))dt + w_{f,1}, \\
 x_{2,t+1} &= x_{2,t} + (V \sin x_{3,t} + W_2(x_{1,t}, x_{2,t}))dt + w_{f,2}, \\
 x_{3,t+1} &= x_{3,t} + \frac{g \tan x_{4,t}}{V}dt + w_{f,3}, \\
 x_{4,t+1} &= x_{4,t} + u_t dt + w_{f,4}, \\
 y_{1,t} &= x_{1,t} + w_{g,1}, \\
 y_{2,t} &= x_{2,t} + w_{g,2},
 \end{aligned} \tag{38}$$

where $[x_1, x_2]$, V , x_3 and x_4 are the position, air speed, heading angle and bank angle of the UAV, respectively. Gravity acceleration is denoted as g . The time interval between two successive states is set as $dt = 0.1$. W_1 and W_2 are wind magnitude for the x and y direction. The wind cannot be directly observed and its effect on the dynamics is assumed unknown. A UAV can only measure its position information from a Global Positioning System (GPS) signal, which inherently contains noise [41]. The cost function and weights are given by:

$$\begin{aligned}
 Q_T = Q &= 2\mathbf{I}, \quad \tilde{Q}_T = \mathbf{0}, \quad R = 100, \quad \text{and} \\
 \alpha(\mu_t) &= (\sqrt{\mu_{1,t}^2 + \mu_{2,t}^2} - R_{des})^2,
 \end{aligned} \tag{39}$$

where R_{des} is the radius of rotation of the circle centered on the origin that the UAV should track continuously. We used the dynamics that exclude unknown wind field

information as the mean prior of the GPSSM. Among the results of the Bayesian filtered state estimation, the results of 2-second intervals and the measurements obtained during the last 4 seconds are stored in memory and the old ones are removed. Online learning is performed for two mini-batch training sets consisting of 20 data points at 0.1 second intervals. The planning horizon for trajectory optimization was set to 6 seconds and the control horizon was set to 1 second. Model learning and trajectory optimization are performed concurrently. Specifically, trajectory optimization is performed using a system model represented by recently updated hyperparameters.

To see the effectiveness of the proposed online learning and planning algorithm, we compared the algorithm with the belief space iLQG [28] in the same environment. The belief space iLQG computes and executes the control inputs in the same RHC scheme as the proposed framework without knowing the influence of the wind. Fig. 4 shows some snapshots of the resulting trajectories obtained when both algorithms were executed. The belief space iLQG combined with the RHC scheme continually reflects changes in the position of the UAV to generate the control inputs. However, an inaccurate system model causes a difference between the planned trajectory and the actual trajectory, which eventually hinders performance of the given task (see Fig. 4(a)-(b)). On the other hand, as shown in Fig. 4(c)-(d), the proposed framework learns the system model in an

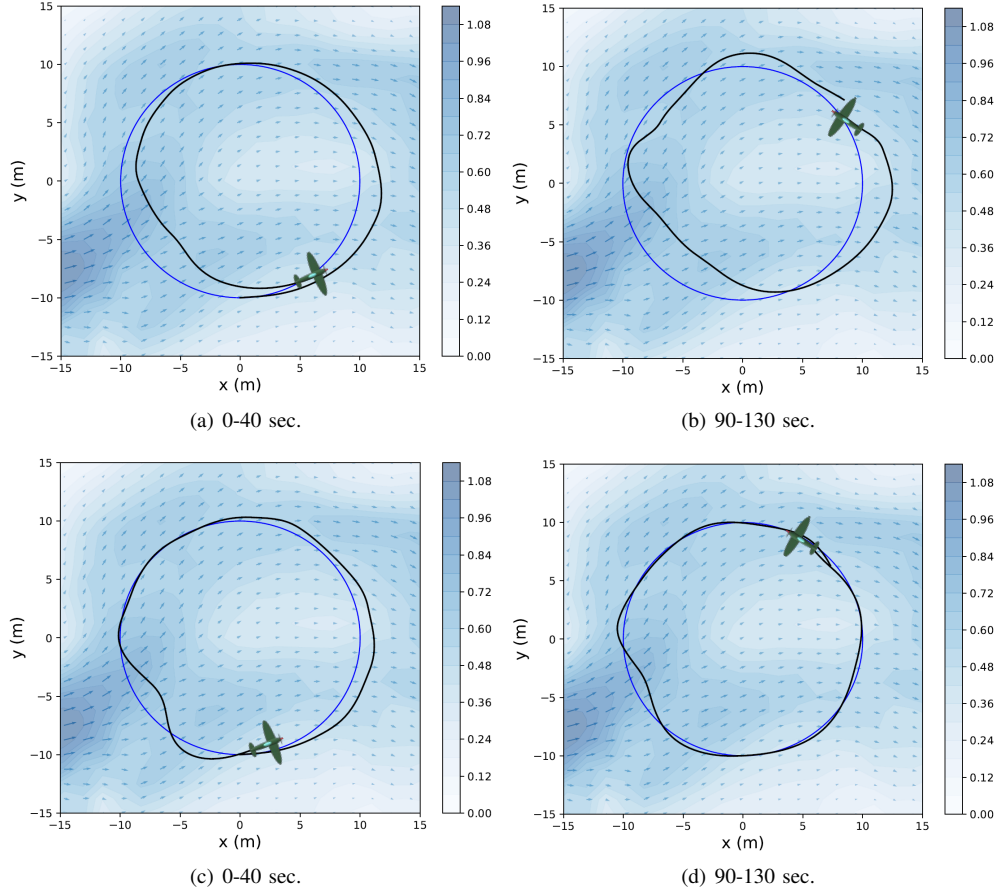


Fig. 4: Resulting trajectories from (a)-(b) belief space iLQG [28] and (c)-(d) proposed algorithm; the blue line shows the reference trajectory that UAV should track continuously and the black line represents the trajectory through which the UAV passes.

online manner using measurements and state estimation results that are obtained while interacting with an unknown environment, thus improving performance when the given task is repeated.

VII. CONCLUSION

In this paper, we proposed an online inference method for learning GPSSM (onlineGPSSM) that fuses stochastic variational inference (VI) and online VI. The onlineGPSSM was shown to not only mitigate computation time issues without catastrophic forgetting, but also support adaptation to changes in a system and/or environment. By integrating the onlineGPSSM with trajectory optimization and Bayesian filtering algorithms, the GPSSM-based reinforcement learning (RL) framework has been developed, which can generate a robust control policy for control/planning. Numerical experiments were presented to demonstrate the applicability and validity of the onlineGPSSM and GPSSM-based RL framework.

REFERENCES

- [1] E. N. Brown, L. M. Frank, D. Tang, M. C. Quirk, and M. A. Wilson, "A statistical paradigm for neural spike train decoding applied to position prediction from ensemble firing patterns of rat hippocampal place cells," *Journal of Neuroscience*, vol. 18, no. 18, pp. 7411–7425, 1998.
- [2] A. S. Polydoros and L. Nalpantidis, "Survey of model-based reinforcement learning: Applications on robotics," *Journal of Intelligent & Robotic Systems*, vol. 86, no. 2, pp. 153–173, 2017.
- [3] L. Ljung, "System identification," in *Signal analysis and prediction*. Springer, 1998, pp. 163–173.
- [4] S. Eleftheriadis, T. Nicholson, M. Deisenroth, and J. Hensman, "Identification of gaussian process state space models," in *Advances in Neural Information Processing Systems*, 2017, pp. 5309–5319.
- [5] J. Ko and D. Fox, "Gp-bayesfilters: Bayesian filtering using gaussian process prediction and observation models," *Autonomous Robots*, vol. 27, no. 1, pp. 75–90, 2009.
- [6] J. Boedecker, J. T. Springenberg, J. Wülfing, and M. Riedmiller, "Approximate real-time optimal control based on sparse gaussian process models," in *Adaptive Dynamic Programming and Reinforcement Learning (ADPRL)*, 2014 *IEEE Symposium on*. IEEE, 2014, pp. 1–8.
- [7] Y. Pan, X. Yan, E. A. Theodorou, and B. Boots, "Prediction under uncertainty in sparse spectrum gaussian processes with

- applications to filtering and control,” in *International Conference on Machine Learning*, 2017, pp. 2760–2768.
- [8] Y. Pan and E. Theodorou, “Probabilistic differential dynamic programming,” in *Advances in Neural Information Processing Systems*, 2014, pp. 1907–1915.
 - [9] M. P. Deisenroth, D. Fox, and C. E. Rasmussen, “Gaussian processes for data-efficient learning in robotics and control,” *IEEE Transactions on Pattern Analysis and Machine Intelligence*, vol. 37, no. 2, pp. 408–423, 2015.
 - [10] R. McAllister and C. E. Rasmussen, “Data-efficient reinforcement learning in continuous state-action gaussian-pomdps,” in *Advances in Neural Information Processing Systems*, 2017, pp. 2037–2046.
 - [11] A. Doerr, C. Daniel, M. Schiegg, D. Nguyen-Tuong, S. Schaal, M. Toussaint, and S. Trimpe, “Probabilistic recurrent state-space models,” *arXiv preprint arXiv:1801.10395*, 2018.
 - [12] W. Sternberg and M. P. Deisenroth, “Identification of gaussian process state-space models,” 2017.
 - [13] A. Svensson and T. B. Schön, “A flexible state-space model for learning nonlinear dynamical systems,” *Automatica*, vol. 80, pp. 189–199, 2017.
 - [14] R. Frigola, Y. Chen, and C. E. Rasmussen, “Variational gaussian process state-space models,” in *Advances in Neural Information Processing Systems*, 2014, pp. 3680–3688.
 - [15] R. Frigola, F. Lindsten, T. B. Schön, and C. E. Rasmussen, “Identification of gaussian process state-space models with particle stochastic approximation em,” *IFAC Proceedings Volumes*, vol. 47, no. 3, pp. 4097–4102, 2014.
 - [16] J. Kober, J. A. Bagnell, and J. Peters, “Reinforcement learning in robotics: A survey,” *The International Journal of Robotics Research*, vol. 32, no. 11, pp. 1238–1274, 2013.
 - [17] D. Mitrovic, S. Klanke, and S. Vijayakumar, “Adaptive optimal feedback control with learned internal dynamics models,” in *From Motor Learning to Interaction Learning in Robots*. Springer, 2010, pp. 65–84.
 - [18] J. Morimoto, G. Zeglin, and C. G. Atkeson, “Minimax differential dynamic programming,” in *SICE Annual Conference Program and Abstracts SICE Annual Conference 2003*. The Society of Instrument and Control Engineers, 2003, pp. 106–106.
 - [19] C. Xie, S. Patil, T. Moldovan, S. Levine, and P. Abbeel, “Model-based reinforcement learning with parametrized physical models and optimism-driven exploration,” in *Robotics and Automation (ICRA), 2016 IEEE International Conference on*. IEEE, 2016, pp. 504–511.
 - [20] T. M. Moldovan, S. Levine, M. I. Jordan, and P. Abbeel, “Optimism-driven exploration for nonlinear systems,” in *Robotics and Automation (ICRA), 2015 IEEE International Conference on*. IEEE, 2015, pp. 3239–3246.
 - [21] T. Broderick, N. Boyd, A. Wibisono, A. C. Wilson, and M. I. Jordan, “Streaming variational bayes,” in *Advances in Neural Information Processing Systems*, 2013, pp. 1727–1735.
 - [22] H. Salimbeni and M. Deisenroth, “Doubly stochastic variational inference for deep gaussian processes,” in *Advances in Neural Information Processing Systems*, 2017, pp. 4588–4599.
 - [23] Z. Ghahramani and H. Attias, “Online variational bayesian learning,” in *Slides from talk presented at NIPS workshop on Online Learning*, 2000.
 - [24] M.-A. Sato, “Online model selection based on the variational bayes,” *Neural computation*, vol. 13, no. 7, pp. 1649–1681, 2001.
 - [25] D. P. Kingma and M. Welling, “Auto-encoding variational bayes,” *arXiv preprint arXiv:1312.6114*, 2013.
 - [26] C. V. Nguyen, Y. Li, T. D. Bui, and R. E. Turner, “Variational continual learning,” *arXiv preprint arXiv:1710.10628*, 2017.
 - [27] T. D. Bui, C. Nguyen, and R. E. Turner, “Streaming sparse gaussian process approximations,” in *Advances in Neural Information Processing Systems*, 2017, pp. 3301–3309.
 - [28] J. Van Den Berg, S. Patil, and R. Alterovitz, “Motion planning under uncertainty using iterative local optimization in belief space,” *The International Journal of Robotics Research*, vol. 31, no. 11, pp. 1263–1278, 2012.
 - [29] R. Frigola-Alcade, “Bayesian time series learning with gaussian processes,” *University of Cambridge*, 2015.
 - [30] C. E. Rasmussen, “Gaussian processes in machine learning,” in *Advanced lectures on machine learning*. Springer, 2004, pp. 63–71.
 - [31] M. Titsias, “Variational learning of inducing variables in sparse gaussian processes,” in *Artificial Intelligence and Statistics*, 2009, pp. 567–574.
 - [32] J. Q. Candela, A. Girard, J. Larsen, and C. E. Rasmussen, “Propagation of uncertainty in bayesian kernel models-application to multiple-step ahead forecasting,” in *Acoustics, Speech, and Signal Processing, 2003. Proceedings.(ICASSP’03). 2003 IEEE International Conference on*, vol. 2. IEEE, 2003, pp. II–701.
 - [33] E. Solak, R. Murray-Smith, W. E. Leithead, D. J. Leith, and C. E. Rasmussen, “Derivative observations in gaussian process models of dynamic systems,” in *Advances in neural information processing systems*, 2003, pp. 1057–1064.
 - [34] Z. Chen *et al.*, “Bayesian filtering: From kalman filters to particle filters, and beyond,” *Statistics*, vol. 182, no. 1, pp. 1–69, 2003.
 - [35] E. Todorov and W. Li, “A generalized iterative lqg method for locally-optimal feedback control of constrained nonlinear stochastic systems,” in *American Control Conference, 2005. Proceedings of the 2005*. IEEE, 2005, pp. 300–306.
 - [36] D. H. Jacobson and D. Q. Mayne, “Differential dynamic programming,” 1970.
 - [37] A. K. Majumdar, *Advanced Free Space Optics (FSO): A Systems Approach*. Springer, 2014, vol. 186.
 - [38] J. Everaerts *et al.*, “The use of unmanned aerial vehicles (uavs) for remote sensing and mapping,” *The International Archives of the Photogrammetry, Remote Sensing and Spatial Information Sciences*, vol. 37, no. 2008, pp. 1187–1192, 2008.
 - [39] J. A. Guerrero, J.-A. Escareño, and Y. Bestaoui, “Quad-rotor mav trajectory planning in wind fields,” in *2013 IEEE International Conference on Robotics and Automation*. IEEE, 2013, pp. 778–783.
 - [40] W. H. Al-Sabban, L. F. Gonzalez, and R. N. Smith, “Wind-energy based path planning for unmanned aerial vehicles using markov decision processes,” in *2013 IEEE International Conference on Robotics and Automation*. IEEE, 2013, pp. 784–789.
 - [41] P. Misra and P. Enge, “Global positioning system: signals, measurements and performance second edition,” *Massachusetts: Ganga-Jamuna Press*, 2006.

APPENDIX A. DERIVATION OF THE EVIDENCE LOWER BOUND (ELBO)

The full joint distribution of the GPSSM is given by:

$$p(\mathbf{y}, \mathbf{x}, \mathbf{f} \mid \vartheta) = p(\mathbf{x}_0) \left[\prod_{t=1}^T p(\mathbf{x}_t \mid \mathbf{f}_t^{\neq \mathbf{z}}) \right] \left[\prod_{t=1}^T \prod_{d=1}^D p(f_{t,d}^{\neq \mathbf{z}_d} \mid \tilde{\mathbf{x}}_{t-1}, \mathbf{z}_d) p(\mathbf{z}_d) \right] \left[\prod_{t=0}^T p(\mathbf{y}_t \mid \mathbf{x}_t) \right]. \quad (40)$$

With the approximate distribution for the variational posterior defined in (11), the variational distribution is defined by:

$$q(\mathbf{x}, \mathbf{f} \mid \vartheta) = q(\mathbf{x}_0) \left[\prod_{t=1}^T p(\mathbf{x}_t \mid \mathbf{f}_t^{\neq \mathbf{z}}) \right] \left[\prod_{t=1}^T \prod_{d=1}^D p(f_{t,d}^{\neq \mathbf{z}_d} \mid \tilde{\mathbf{x}}_{t-1}, \mathbf{z}_d) q(\mathbf{z}_d) \right]. \quad (41)$$

Based on equations (40) and (41), the ELBO is derived by:

$$\begin{aligned} \log p(\mathbf{y} \mid \vartheta) &\geq \mathbb{E}_{q(\mathbf{x}, \mathbf{f} \mid \vartheta)} \left[\log \frac{p(\mathbf{y}, \mathbf{x}, \mathbf{f} \mid \vartheta)}{q(\mathbf{x}, \mathbf{f} \mid \vartheta)} \right] \\ &= \mathbb{E}_{q(\mathbf{x}, \mathbf{f} \mid \vartheta)} \left[\log \frac{p(\mathbf{x}_0) \left[\prod_{t=1}^T p(\mathbf{x}_t \mid \mathbf{f}_t^{\neq \mathbf{z}}) \right] \left[\prod_{t=1}^T \prod_{d=1}^D p(f_{t,d}^{\neq \mathbf{z}_d} \mid \tilde{\mathbf{x}}_{t-1}, \mathbf{z}_d) p(\mathbf{z}_d) \right] \left[\prod_{t=0}^T p(\mathbf{y}_t \mid \mathbf{x}_t) \right]}{q(\mathbf{x}_0) \left[\prod_{t=1}^T p(\mathbf{x}_t \mid \mathbf{f}_t^{\neq \mathbf{z}}) \right] \left[\prod_{t=1}^T \prod_{d=1}^D p(f_{t,d}^{\neq \mathbf{z}_d} \mid \tilde{\mathbf{x}}_{t-1}, \mathbf{z}_d) q(\mathbf{z}_d) \right]} \right] \\ &= \mathbb{E}_{q(\mathbf{x}, \mathbf{f} \mid \vartheta)} \left[\log \frac{p(\mathbf{x}_0) \left[\prod_{d=1}^D p(\mathbf{z}_d) \right] \left[\prod_{t=0}^T p(\mathbf{y}_t \mid \mathbf{x}_t) \right]}{q(\mathbf{x}_0) \left[\prod_{d=1}^D q(\mathbf{z}_d) \right]} \right] \\ &= \mathbb{E}_{q(\mathbf{x}, \mathbf{f} \mid \vartheta)} \left[\log \prod_{t=0}^T p(\mathbf{y}_t \mid \mathbf{x}_t) \right] - \mathbb{E}_{q(\mathbf{x}, \mathbf{f} \mid \vartheta)} \left[\log \frac{q(\mathbf{x}_0)}{p(\mathbf{x}_0)} \right] - \mathbb{E}_{q(\mathbf{x}, \mathbf{f} \mid \vartheta)} \left[\sum_{d=1}^D \log \frac{q(\mathbf{z}_d)}{p(\mathbf{z}_d)} \right] \\ &= \mathbb{E}_{q(\mathbf{x}_0, \mathbf{f})} \left[\log \prod_{t=0}^T p(\mathbf{y}_t \mid \mathbf{x}_t) \right] - \mathbb{E}_{q(\mathbf{x}_0)} \left[\log \frac{q(\mathbf{x}_0)}{p(\mathbf{x}_0)} \right] - \mathbb{E}_{q(\mathbf{z})} \left[\sum_{d=1}^D \log \frac{q(\mathbf{z}_d)}{p(\mathbf{z}_d)} \right] \\ &= \sum_{t=0}^T \mathbb{E}_{q(\mathbf{x}_t)} [\log p(\mathbf{y}_t \mid \mathbf{x}_t)] - \mathcal{D}_{KL}(q(\mathbf{x}_0) \parallel p(\mathbf{x}_0)) - \sum_{d=1}^D \mathcal{D}_{KL}(q(\mathbf{z}_d) \parallel p(\mathbf{z}_d)). \end{aligned} \quad (42)$$

For a more detailed explanation, refer to [11,22] and the references therein.

APPENDIX B. DERIVATION OF THE NEGATIVE ELBO

The new approximate posterior $q(\mathbf{x}, \mathbf{f} \mid \vartheta') = p(\mathbf{x}, \mathbf{f}^{\neq \mathbf{b}} \mid \mathbf{b}, \theta') q'(\mathbf{b}) q(\mathbf{x}_0')$ can be obtained by minimizing the KL divergence:

$$\mathcal{D}_{KL}(q(\mathbf{x}, \mathbf{f} \mid \vartheta') \parallel \hat{p}(\mathbf{x}, \mathbf{f} \mid \mathbf{y}, \mathbf{y}', \vartheta')) = \log \frac{p(\mathbf{y}, \mathbf{y}' \mid \vartheta')}{p(\mathbf{y} \mid \vartheta)} + \mathbb{E}_{q(\mathbf{x}, \mathbf{f} \mid \vartheta')} \left[\log \frac{q(\mathbf{x}, \mathbf{f} \mid \vartheta')}{p(\mathbf{x}, \mathbf{f} \mid \vartheta') p(\mathbf{y}' \mid \mathbf{x}) \frac{q(\mathbf{x}, \mathbf{f} \mid \vartheta)}{p(\mathbf{x}, \mathbf{f} \mid \vartheta)}} \right]. \quad (43)$$

Since the KL divergence is non-negative, the second term in (43) is the negative approximate lower bound of the log marginal likelihood. Thus, the negative evidence lower bound (negative ELBO) of the approximate online log marginal likelihood is represented by:

$$\begin{aligned} \mathcal{NL}(\vartheta') &= \mathbb{E}_{q(\mathbf{x}, \mathbf{f} \mid \vartheta')} \left[\log \frac{q(\mathbf{x}, \mathbf{f} \mid \vartheta')}{p(\mathbf{x}, \mathbf{f} \mid \vartheta') p(\mathbf{y}' \mid \mathbf{x}) \frac{q(\mathbf{x}, \mathbf{f} \mid \vartheta)}{p(\mathbf{x}, \mathbf{f} \mid \vartheta)}} \right] \\ &= \mathbb{E}_{q(\mathbf{x}, \mathbf{f} \mid \vartheta')} \left[\log \frac{q(\mathbf{x}, \mathbf{f} \mid \vartheta')}{p(\mathbf{x}, \mathbf{f} \mid \vartheta') p(\mathbf{y}' \mid \mathbf{x})} \right] + \mathbb{E}_{q(\mathbf{x}, \mathbf{f} \mid \vartheta')} \left[\log \frac{p(\mathbf{x}, \mathbf{f} \mid \vartheta)}{q(\mathbf{x}, \mathbf{f} \mid \vartheta)} \right]. \end{aligned} \quad (44)$$

The first term of (44) is obtained in the same way as in (42). From equations (9) and (41), $p(\mathbf{x}, \mathbf{f} \mid \vartheta)/q(\mathbf{x}, \mathbf{f} \mid \vartheta)$ in the last term of (44) is given by:

$$\frac{p(\mathbf{x}, \mathbf{f} \mid \vartheta)}{q(\mathbf{x}, \mathbf{f} \mid \vartheta)} = \frac{p(\mathbf{x}_0) \left[\prod_{t=1}^T \overline{p(\mathbf{x}_t \mid \mathbf{f}_t^{\neq \mathbf{a}})} \right] \left[\prod_{t=1}^T \prod_{d=1}^D \overline{p(\mathbf{f}_{t,d}^{\neq \mathbf{a}_d} \mid \tilde{\mathbf{x}}_{t-1}, \mathbf{a}_d, \theta_d)} p(\mathbf{a}_d \mid \theta_d) \right]}{q(\mathbf{x}_0) \left[\prod_{t=1}^T \overline{p(\mathbf{x}_t \mid \mathbf{f}_t^{\neq \mathbf{a}})} \right] \left[\prod_{t=1}^T \prod_{d=1}^D \overline{p(\mathbf{f}_{t,d}^{\neq \mathbf{a}_d} \mid \tilde{\mathbf{x}}_{t-1}, \mathbf{a}_d, \theta_d)} q(\mathbf{a}_d) \right]} = \frac{p(\mathbf{x}_0) \prod_{d=1}^D p(\mathbf{a}_d \mid \theta_d)}{q(\mathbf{x}_0) \prod_{d=1}^D q(\mathbf{a}_d)}. \quad (45)$$

Substituting this, the last term of (44) is given by:

$$\begin{aligned} & \iint q(\mathbf{x}, \mathbf{f} \mid \vartheta') \left[\log \frac{p(\mathbf{x}, \mathbf{f} \mid \vartheta)}{q(\mathbf{x}, \mathbf{f} \mid \vartheta)} \right] d\mathbf{x} d\mathbf{f} \\ &= \iint p(\mathbf{x}, \mathbf{f}^{\neq \mathbf{b}} \mid \mathbf{b}, \theta') q'(\mathbf{b}) q(\mathbf{x}'_0) \left[\log \frac{p(\mathbf{x}_0) \prod_{d=1}^D p(\mathbf{a}_d \mid \theta_d)}{q(\mathbf{x}_0) \prod_{d=1}^D q(\mathbf{a}_d)} \right] d\mathbf{x} d\mathbf{f} \\ &= \iint p(\mathbf{x} \mid \mathbf{f}^{\neq \mathbf{b}}, \mathbf{b}, \theta') p(\mathbf{f}^{\neq \mathbf{b}} \mid \mathbf{b}, \theta') q'(\mathbf{b}) q(\mathbf{x}'_0) \left[\log \frac{p(\mathbf{x}_0)}{q(\mathbf{x}_0)} + \log \frac{\prod_{d=1}^D p(\mathbf{a}_d \mid \theta_d)}{\prod_{d=1}^D q(\mathbf{a}_d)} \right] d\mathbf{x} d\mathbf{f} \\ &= \int p(\mathbf{x} \mid \mathbf{f}^{\neq \mathbf{b}}, \mathbf{b}, \theta') q(\mathbf{x}'_0) \left[\log \frac{p(\mathbf{x}_0)}{q(\mathbf{x}_0)} \right] d\mathbf{x} + \int p(\mathbf{f}^{\neq \mathbf{b}} \mid \mathbf{b}, \theta') q'(\mathbf{b}) \left[\log \frac{\prod_{d=1}^D p(\mathbf{a}_d \mid \theta_d)}{\prod_{d=1}^D q(\mathbf{a}_d)} \right] d\mathbf{f} \quad (46) \\ &= \int q(\mathbf{x}'_0) \log \frac{p(\mathbf{x}_0)}{q(\mathbf{x}_0)} d\mathbf{x} + \sum_{d=1}^D \int q'(\mathbf{a}_d) \log \frac{p(\mathbf{a}_d \mid \theta_d)}{q(\mathbf{a}_d)} d\mathbf{a}_d \\ &= \int q(\mathbf{x}'_0) \log \frac{p(\mathbf{x}_0)}{q(\mathbf{x}_0)} d\mathbf{x} + \sum_{d=1}^D \int q'(\mathbf{a}_d) \left(\log \frac{q'(\mathbf{a}_d)}{q(\mathbf{a}_d)} + \log \frac{p(\mathbf{a}_d \mid \theta_d)}{q'(\mathbf{a}_d)} \right) d\mathbf{a}_d \\ &= \int q(\mathbf{x}'_0) \log \frac{p(\mathbf{x}_0)}{q(\mathbf{x}_0)} d\mathbf{x} + \sum_{d=1}^D \mathcal{D}_{KL}(q'(\mathbf{a}_d) \parallel q(\mathbf{a}_d)) - \sum_{d=1}^D \mathcal{D}_{KL}(q'(\mathbf{a}_d) \parallel p(\mathbf{a}_d \mid \theta_d)), \end{aligned}$$

where

$$\begin{aligned} q'(\mathbf{a}_d) &= \int p(\mathbf{a}_d \mid \mathbf{b}_d, \theta'_d) q'(\mathbf{b}_d) d\mathbf{b}_d \\ &= \int \mathcal{N}(\mathbf{a}_d; \mathbf{m}_{\mathbf{a}_d \mid \mathbf{b}_d}, \mathbf{S}_{\mathbf{a}_d \mid \mathbf{b}_d}) \mathcal{N}(\mathbf{b}_d; \boldsymbol{\mu}_{\mathbf{b},d}, \boldsymbol{\Sigma}_{\mathbf{b},d}) d\mathbf{b}_d \\ &= \mathcal{N}(\mathbf{a}_d; \mathbf{m}_{\boldsymbol{\eta}_d} + \mathbf{K}_{\boldsymbol{\eta}_d \boldsymbol{\eta}'_d} \mathbf{K}_{\boldsymbol{\eta}'_d \boldsymbol{\eta}'_d}^{-1} [\boldsymbol{\mu}_{\mathbf{b},d} - \mathbf{m}_{\boldsymbol{\eta}'_d}], \mathbf{S}_{\mathbf{a}_d \mid \mathbf{b}_d} + \mathbf{K}_{\boldsymbol{\eta}_d \boldsymbol{\eta}'_d} \mathbf{K}_{\boldsymbol{\eta}'_d \boldsymbol{\eta}'_d}^{-1} \boldsymbol{\Sigma}_{\mathbf{b},d} \mathbf{K}_{\boldsymbol{\eta}'_d \boldsymbol{\eta}'_d}^{-1} \mathbf{K}_{\boldsymbol{\eta}_d \boldsymbol{\eta}_d}), \quad (47) \\ p(\mathbf{a}_d \mid \mathbf{b}_d, \theta'_d) &= \mathcal{N}(\mathbf{a}_d; \mathbf{m}_{\mathbf{a}_d \mid \mathbf{b}_d}, \mathbf{S}_{\mathbf{a}_d \mid \mathbf{b}_d}) \\ &= \mathcal{N}(\mathbf{a}_d; \mathbf{m}_{\boldsymbol{\eta}_d} + \mathbf{K}_{\boldsymbol{\eta}_d \boldsymbol{\eta}'_d} \mathbf{K}_{\boldsymbol{\eta}'_d \boldsymbol{\eta}'_d}^{-1} [\mathbf{b}_d - \mathbf{m}_{\boldsymbol{\eta}'_d}], \mathbf{K}_{\boldsymbol{\eta}_d \boldsymbol{\eta}_d} - \mathbf{K}_{\boldsymbol{\eta}_d \boldsymbol{\eta}'_d} \mathbf{K}_{\boldsymbol{\eta}'_d \boldsymbol{\eta}'_d}^{-1} \mathbf{K}_{\boldsymbol{\eta}'_d \boldsymbol{\eta}_d}), \\ q(\mathbf{b}_d) &= \mathcal{N}(\mathbf{b}_d; \boldsymbol{\mu}_{\mathbf{b},d}, \boldsymbol{\Sigma}_{\mathbf{b},d}). \end{aligned}$$

The first term in (46) can be neglected if the initial state is sufficiently broad. Thus, the negative evidence lower bound (negative ELBO) of the approximate online log marginal likelihood is represented by:

$$\begin{aligned} \mathcal{NL}(\vartheta') &= - \sum_{t=0}^T \mathbb{E}_{q(\mathbf{x}_t)} [\log p(\mathbf{y}_t \mid \mathbf{x}_t)] + \mathcal{D}_{KL}(q(\mathbf{x}'_0) \parallel p(\mathbf{x}'_0)) + \sum_{d=1}^D \mathcal{D}_{KL}(q'(\mathbf{b}_d) \parallel p(\mathbf{b}_d \mid \theta'_d)) \\ &\quad + \sum_{d=1}^D \mathcal{D}_{KL}(q'(\mathbf{a}_d) \parallel q(\mathbf{a}_d)) - \sum_{d=1}^D \mathcal{D}_{KL}(q'(\mathbf{a}_d) \parallel p(\mathbf{a}_d \mid \theta_d)). \end{aligned} \quad (48)$$